



City Research Online

City, University of London Institutional Repository

Citation: Papadopoulos, Konstantinos, Gavaises, M. & Atkin, C. (2014). A simplified mathematical model for thrombin generation. *Medical Engineering and Physics*, 36(2), pp. 196-204. doi: 10.1016/j.medengphy.2013.10.012

This is the accepted version of the paper.

This version of the publication may differ from the final published version.

Permanent repository link: <https://openaccess.city.ac.uk/id/eprint/13568/>

Link to published version: <https://doi.org/10.1016/j.medengphy.2013.10.012>

Copyright: City Research Online aims to make research outputs of City, University of London available to a wider audience. Copyright and Moral Rights remain with the author(s) and/or copyright holders. URLs from City Research Online may be freely distributed and linked to.

Reuse: Copies of full items can be used for personal research or study, educational, or not-for-profit purposes without prior permission or charge. Provided that the authors, title and full bibliographic details are credited, a hyperlink and/or URL is given for the original metadata page and the content is not changed in any way.

City Research Online:

<http://openaccess.city.ac.uk/>

publications@city.ac.uk

A simplified mathematical model for thrombin generation

Papadopoulos Kostis, Gavaises Manolis and Chris Atkin
School of Engineering and Mathematical Sciences

City University London

Northampton square, London

EC1V 0HB

Room: C171

Phone: +44 (0) 20 7040 8115

Fax: +44 (0) 20 7040 8566

Email: Papadopoulos.Konstantinos.1@city.ac.uk :
M.Gavaises@city.ac.uk

3 **Abstract**

4 A new phenomenological mathematical model based directly on laboratory data for thrombin
5 generation and having a patient-specific character is described. A set of the solved equations
6 for cell-based models of blood coagulation that can reproduce the temporal evolution of
7 thrombin generation is proposed; such equations are appropriate for use in Computational
8 Fluid Dynamics (CFD) simulations. The initial values for the reaction rates are either taken
9 from already existing model or experimental data, or they can be obtained from simple
10 reasoning under certain assumptions; it is shown that coefficients can be adjusted in order to
11 fit a range of different thrombin generation curves as derived from thrombin generation
12 assays. The behaviour of the model for different platelet concentration seems to be in good
13 agreement with reported experimental data. It is shown that the reduced set of equations used
14 represents to a good approximation a low-order model of the detailed mechanism and thus it
15 can represent a cost-effective and-case specific mathematical model of coagulation reactions
16 up to thrombin generation

17 **Keywords:**

18 CFD, coagulation, simulation, thrombus

19

20 **Introduction**

21 The formation of thrombus in blood is involved in a number of life threatening situations like
22 Coronary Artery Disease and mechanical heart valve complications; it is a multi-scale
23 phenomenon both in respect of time and space, involving a number of biochemical
24 substances, blood circulating minerals and cellular responses. While the formation of blood
25 clot is a physiological response of human body to vessel injury, it can be initiated when blood

Papadopoulos et al-Model for thrombin generation

26 contacts certain substances like those exposed after the rupture of atheromatous plaques in
27 stenosed vessels [Rauch, Osende et al. 2001] and when pathological flow conditions prevail
28 in a region [Nesbitt, Westein et al. 2009]. Between the initiation and the formation of a
29 thrombus, a series of enzymatic reactions takes place also known as coagulation cascade
30 [Furie and Furie 2008], classically divided in three parts: (1) the extrinsic or Tissue Factor
31 (TF) pathway, (2) the intrinsic or contact pathway and the (3) common pathway. In every
32 step of the process a circulating zymogen is activated, with the activation reaction being
33 catalysed by the products of previous steps. However, as most of these enzymatic reactions
34 take place on cell membranes, the current approaches for coagulation are cell-based models
35 and the process is divided in three discrete phases, initiation, amplification and propagation.
36 Thrombin (factor IIa) and platelets play critical roles in the coagulation process. Thrombin in
37 the final step catalyses the conversion of fibrinogen (factor I) to fibrin (factor Ia), a protein
38 that through polymerization creates a mesh clot that also traps circulating blood cells. In
39 addition, thrombin activates factor XIII (that forms bonds that crosslink the fibrin strands
40 [Mosesson 2005]), causes the activation of platelets [Brass 2003], the activation of factors V
41 and VIII and their inhibitor protein C (APC). Platelets on the other hand, after activation by
42 chemical or mechanical stimulation [Jesty, Yin et al. 2003] become adhesive and form
43 aggregates on the materials exposed after arterial damage [Badimon, Badimon et al. 1986] or
44 plaque rupture [Fernández-Ortiz, Badimon et al. 1994; Reininger, Bernlochner et al. 2010] or
45 in flowing blood. In addition they play a major role in thrombin formation [Rosing, van Rijn
46 et al. 1985; Monroe, Hoffman et al. 2002] and they enhance the coagulation process by
47 supporting on their membrane some of the coagulation reactions [Smith 2009], releasing
48 chemical substances and micro-particles [Rendu and Brohard-Bohn 2001] that influence the
49 progress of coagulation and activate other platelets.

50 The advance of computational techniques and increase of computational power have made

Papadopoulos et al-Model for thrombin generation

51 possible the emergence of in silico studies that reproduce a part of or the whole process in
52 greater or lesser detail, simulating either the whole process of thrombus formation or only the
53 coagulation reaction system up to thrombin or fibrin production. The first mathematical
54 simulation of thrombin and fibrin generation in plasma used exponential time functions as
55 fixed inputs for concentration of some enzymes [Willems, Lindhout et al. 1991]. In vitro
56 measurements of the reaction rate constants [Lawson, Kalafatis et al. 1994] were used for the
57 development of a system of 20 reactions, including formation and breakage of complexes, in
58 a study that mainly focused on the effect of variation of the concentration of different factors
59 [Jones and Mann 1994]. A similar model was proposed for the intrinsic pathway including
60 fibrin production and APC inhibition mechanism, and was used to investigate threshold
61 values for some enzymes and the spatial propagation of coagulation from the reacting site due
62 to diffusion [Zarnitsina, Pokhilko et al. 1996; Zarnitsina, Pokhilko et al. 1996]. Subsequent
63 work included more chemical substances and biochemical processes [Hockin, Jones et al.
64 2002] up to thrombin production, resulting in a system consisting of 27 reactions and 42
65 reaction rate constants that later was combined with a Monte Carlo simulation method, in
66 order to detect changes to the cascade initiation behaviour, due to small variation of the
67 concentration of enzymes induced by the stochastic approach [Lo, Denney et al. 2005]. At the
68 same time some studies used simulations to investigate a specific part of the coagulation
69 cascade, as the function of positive feedback loops and threshold concentrations for cascade
70 initiation [Beltrami and Jesty 1995], the triggering threshold with respect to Tissue Factor
71 Pathway Inhibitor (TFPI) [Xu, Hu Xu et al. 2005] or the inhibition mechanism of APC [Qiao,
72 Xu et al. 2004].

73 The studies that simulate thrombus formation and growth, simultaneously with blood flow
74 and concentration of related substances, necessitate a less detailed sub-model for the
75 coagulation cascade. While for the first studies of this kind the production rates of substances

Papadopoulos et al-Model for thrombin generation

76 were mainly modelled as fluxes or with the use of few reactions [Hubbell and McIntire 1986;
77 Folie and McIntire 1989], the increase of computational power allowed more complicated
78 multi-scale and multi-phase models to emerge, that include an integrated coagulation sub-
79 model. The authors of [Kuharsky and Fogelson 2001] proposed an integrated model of
80 thrombus formation under flow conditions, taking into account the localization of reactions
81 on surfaces, with the inclusion of the available binding sites on cell membranes for enzymes
82 and using a system of 59 equations to simulate the coagulation system up to thrombin
83 generation. A study that modelled platelet-platelet and platelet-wall interaction as reversible
84 elastic links demonstrated the influence of these interactions on the flow field and predicted
85 thrombus evolution and emboli formation [Fogelson and Guy 2004]. The initial model was
86 later improved with the addition of the APC mechanism and the transport of substances
87 between plasma and endothelium cells [Fogelson and Tania 2005]. The same concepts for
88 cells and reactions were combined with an immersed boundary method [Lai and Peskin 2000;
89 Peskin 2002] for modelling platelet movement and the interaction between platelet membrane
90 sites and chemicals or endothelium. The results of this micro-scale model were also used to
91 develop a continuous model for platelet aggregation (with platelets as continuous phase with
92 movement limitations) describing the alterations in blood flow due to the presence of
93 aggregated platelets [Fogelson and Guy 2008]. The macro-scale model was tested in
94 simulations with pulsating flow in an idealized two dimensional vessel bifurcation [Yang,
95 Lewis et al. 2004]. The continuous model, with coupling of flow with thrombus growth and
96 including flow and transport within the thrombus, was used to demonstrate the effects of flow
97 conditions and the quantity of TF exposed in thrombus growth [Leiderman and Fogelson
98 2011]. Anand et al [Anand, Rajagopal et al. 2003; Anand, Rajagopal et al. 2005] presented
99 another multi-process model that used a viscoelastic model to simulate flow for both free
100 vessel lumen and clot. This model also incorporated the activation of platelets due to

101 excessive shear stress and fibrin production and lysis. In a similar work, a model for the
102 viscosity of blood depending on fibrin concentration was proposed and used in a three-
103 dimensional simulation of blood coagulation in a tube with a reacting site; in this study the
104 area where fibrin concentration exceeded a specific value interpreted as the area occupied by
105 the clot[Bodnár and Sequeira 2008]. In [Xu, Chen et al. 2008] another multi-scale model was
106 proposed that included a cellular pot model [Marée, Grieneisen et al. 2007] for discrete cells
107 and cell movement was simulated through an energy-based stochastic process. The
108 simulation involved differentiation of cell movements depending on fibrin levels and cell-cell
109 or cell-surface interaction and bonds. The model was used to evaluate the role of fVII in
110 venous thrombus formation due to vessel injury [Xu, Lioi et al. 2010] and to examine the
111 impact of pulsating flow and the non-Newtonian characteristics of blood on thrombus growth
112 [Xu, Chen et al. 2009].

113 While the detailed description of coagulation included in these works makes them appropriate
114 for studying the influence of different factors, unfortunately it increases dramatically the
115 computational cost; thus published applications mainly refer to small two dimensional
116 regions ($\sim 100\mu\text{m}$) while the dimensions of computational regions for studying thrombus
117 formation in a coronary artery or in mechanical heart valves are much larger (typically, the
118 diameter of the coronary artery is about 4mm while the diameter of the aortic root is of some
119 cm) with the flow distribution being three-dimensional and strongly time dependent
120 preventing use of simplified flow models. In addition, these models do not have patient-
121 specific characteristics, as the use of reaction rate constants derived from experiments do not
122 allow the significant variability of thrombin generation observed for different individuals
123 [Oliver, Monroe et al. 1999]. At the same time, it has been shown that the resulting thrombin
124 generation curve predicted by such models under steady state conditions can be simulated in
125 different ways by a much simpler system of 6 equations [Wagenvoort, Hemker et al. 2006].

126 As the process between the initial stimulation and the formation of thrombin consist the main
127 part of the coagulation reactions, our motivation is to develop a phenomenological model for
128 thrombin formation that would be efficient enough to be used with three dimensional
129 Computational Fluid Dynamic (CFD) simulations while also being adjustable in order to
130 reflect measured differences existing in data of different individuals. A case-specific
131 simplified model like this, though not including the full biochemical details of the process,
132 could be used for comparison of different cases of clinical interest.

133 **Materials and methods**

134 The aim of the study is to propose a set of equations that describe the thrombin generation in
135 blood using the minimum possible number of parameters but which are able to describe with
136 acceptable accuracy the whole process. The model is validated against experimental results
137 for thrombin generation in vitro from Thrombin Generation Assays (TGA). The proposed
138 model for thrombin production is based on the cell-based models of coagulation[Smith 2009];
139 the full description of the biochemical processes are mainly based on [Hoffman and Monroe
140 2001]. For a detailed modelling of coagulation the localization of the different reactions
141 makes the task more complicated, as it requires taking into account additional parameters
142 such as the binding rate of the substances on cell membranes and the expression,
143 concentration and availability of appropriate binding sites on the cell surfaces. For the
144 development of a simplified model however, it can function as an advantage, as the processes
145 can be grouped in respect to the location they occur (on platelet surface, on the vessel wall or
146 in plasma). This approach is rigorous in cases where the transport of reactants is mainly due
147 to convection such as arterial flow conditions, or in cases where the different species are well
148 mixed. The generation of thrombin and generally the coagulation process is mainly attributed
149 to activated platelets, while the initiation phase is localized on the reacting site of the vessel
150 surface. The burst of thrombin generation is considered to occur when the small amounts of

Papadopoulos et al-Model for thrombin generation

151 thrombin produced during the initiation phase cause thrombin concentration to exceed a
152 threshold value. The threshold values used are within the range of thrombin concentration
153 values that have been reported in [Rosing, van Rijn et al. 1985] as being capable of causing
154 platelet activation, 0.5 to 1.2nM of thrombin (0.05 to 0.12U/ml) . The equations of the model
155 are shown in Table 1. The initial values for the reaction rate constants, shown in Table 2, are
156 taken either from already existing models or from experimental studies.

157 As the proposed model used a reduced number of 4 reactions, each reaction rate represents
158 the integral effect of more than one actual process. Also, ‘activated platelets’ actually
159 represent platelet activity, in the sense that 100% activated platelets implies maximum
160 platelet activity rather than the fact that all platelets are activated. Figure 1a illustrates the
161 actual biochemical reactions that influence each constant while Figure 1b the reduced model.
162 The model is structured as follows: During the initiation phase thrombin generation is
163 described by a slow first order reaction. This reaction, which is localized on the TF-bearing
164 cells, is used to describe the whole pro-coagulant activity that occurs on the TF-bearing cells
165 – formation of the TF-VIIa complex, activation of factors IX, X and V. In this reaction is also
166 included the inhibition of the amounts of IXa, Xa that leave the cell surfaces by TFPI in
167 plasma. The initial value for the reaction rate constant was estimated using the lag times
168 reported in [Lawson, Kalafatis et al. 1994; van't Veer and Mann 1997]. Inhibition of thrombin
169 during this phase is also modelled as a first-order reaction, with the value of the reaction rate
170 constant for thrombin inhibition calculated from the IIa · ATIII inhibition reaction, using the
171 initial bulk concentration of ATIII ($k_{in} = k_{in,ATIII} \cdot \varphi_{ATIII,0} = 1.71 \cdot 10^{-2} s^{-1}$), as this
172 reaction is the major process of thrombin inhibition .(Thrombin inactivation is 77% by anti-
173 thrombin, 14% a₂ macroglobulin and 9% by minor inhibitors [Hemker and Béguin 1995]).
174 With this setup for the initiation phase, the model describes the threshold behaviour of the
175 initiation of blood coagulation in respect to TF concentration[Okorie, Denney et al. 2008;

Papadopoulos et al-Model for thrombin generation

176 Shen, Kastrup et al. 2008], as there is a minimum value of activation constant capable of
177 causing thrombin burst and, as this constant is related to the TF concentration (see
178 discussion), a threshold value for TF concentration.

179 Beyond the point that thrombin concentration has reached the threshold value, the conversion
180 of prothrombin to thrombin is mainly attributed to platelets after their activation. This process
181 is modelled as a second-order reaction, with the initial values for the reaction rate constant
182 used from [Rosing, van Rijn et al. 1985; Sorensen, Burgreen et al. 1999]. Platelets can be
183 activated either by thrombin, if its concentration is greater than the threshold value, or
184 directly by other activated platelets. Thrombin in concentration about 1nM can initiate the
185 activation of platelets [Liu, Freedman et al. 1994], from 0.5nM for minimum activity to
186 1.2nM for maximal [Rosing, van Rijn et al. 1985]. Platelet activation by thrombin is
187 modelled as a first-order reaction that is initiated when thrombin concentration reaches the
188 threshold value. The activation of platelets by activated platelets represents the activation by
189 platelet-released substances and is modelled as a second order reaction. the reaction rate
190 constants for the activation of platelets used were found in [Kuharsky and Fogelson 2001]. In
191 the case of TF induced coagulation the contribution of the later reaction is negligible, but it
192 can make the model capable of being used to describe shear induced coagulation.

193

194 Inhibition of thrombin during the propagation phase is again modelled as a first-order
195 reaction. The reaction rate constant for the inhibition of thrombin in plasma is not the same as
196 for the initiation phase; here we must note that this constant is significantly smaller than the
197 one used in [Leiderman and Fogelson 2011] for modelling this reaction in the same manner,
198 which was based on thrombin half-life in plasma. However, as the activation of protein C that
199 acts as an inhibitor to the coagulation process mainly occurs on the endothelium cells, for the

Papadopoulos et al-Model for thrombin generation

200 areas near the endothelium cells the value used for thrombin inhibition is larger, with the
 201 exact value derived from the adjustment of the model with the use of TGA results. As
 202 demonstrated in Figure 2, the model using the initial parameter values gives reasonable
 203 results. By adjusting the values of the constants and parameters of the model within
 204 physiological limits, the model can reproduce, to a good level of accuracy, actual thrombin
 205 production, by considering the four main parameters of a thrombin generation assay: lag-time
 206 (Tlag), maximum concentration (Cmax), time until thrombin concentration reaches the
 207 maximum (Tmax) and the estimated thrombin potential (ETP); the last one is represented by
 208 the surface under the curve in a thrombin concentration vs time graph. The initial attempts of
 209 adjustments were performed manually, but in general the adjustment can be done using the
 210 following procedure and assumptions.

211 Platelet response is very fast compared to the other processes included in the model
 212 [Frojmovic, Mooney et al. 1994; Frojmovic, Mooney et al. 1994]. With the approximation
 213 that all platelets are activated as soon as thrombin concentration reaches the threshold value,
 214 the system of the equations can be analytically solved, giving the equation that describes
 215 thrombin concentration through time. This equation has the general form (see appendix 1a):

$$[IIa](t) = \frac{B_i}{A_i - C_i} (e^{A_i t} - e^{C_i t}) = F(t)$$

216 The equation is similar to the equation proposed in [Wagenvoord, Hemker et al. 2006] but in
 217 a non-uniform platelet distribution the results will vary in space. Here the constants A, B and
 218 C depend both on the model parameters and TAG results, and they have different values for
 219 the initial phase and the propagation phase.

220 Using the parameters of the TGA and this function we obtain the equations

$$F(Tlag) = [IIa]_{thr}$$

$$F(Tmax) = Cmax$$

$$\frac{dF}{dt}(Tmax) = 0$$

$$\int_0^{\infty} F(t)dt \cong \int_{Tlag}^{t\infty} F(t)dt = ETP$$

221 From this set of equations the constants of the model can be approximated numerically,
 222 making the resulting model equations able to reproduce with the curve of a TGA with given
 223 parameters. In most of the following results only the constants related to thrombin production
 224 k_{II}^{AP} , k_{surf} , k_{in} (see Table 1) were adjusted. In case data from the whole curve is available,
 225 the constants can be approximated as described in appendix 1b.

226 **Results**

227 We first applied the model using the initial values for the constants; while the resulting curve
 228 has the shape of a typical thrombin generation curve, the actual values were significantly
 229 higher than the typical results of TGA for fresh platelet rich plasma as reported in
 230 [Gerotziakas, Depasse et al. 2005]. Performing simulations for different time steps, we found
 231 that the results of the model are identical for time steps below 0.5s (Figure 2). As a whole
 232 heart cycle at rest conditions is about 0.8s (for 75 bpm), the maximum magnitude of the time
 233 steps for simulating pulsating flow is much smaller, thus in terms of temporal discretization,
 234 the coupling of the model with CFD simulations can be straightforward.

235 Subsequently we applied the model in 8 different cases, denoted as Case1-8. In the plots,
 236 when both model and experimental results are represented, model results are named ‘C#
 237 model’ and the experimental results ‘C# exp’. The equations for the adjustment of the
 238 constants were solved in MATLAB, while the adjustment of the platelet related constants was
 239 done manually using Excel and Systems Biology Toolbox 2 [2006]. Case 1 represents the

240 tuning of the model constants in order to reproduce typical TGA results as reported in
241 [Gerotziafas, Depasse et al. 2005] and the resulting curve (C1 model) is shown in Figure 3
242 and Figure 4, compared with curves representing slower thrombin generation. In the absence
243 of inhibition (case 2 and case 3), the time interval between the end of the initiation phase and
244 the moment that thrombin concentration reaches its maximum value is 2-4 min, depending on
245 the constant for thrombin activation by activated platelets, and the results match
246 approximately the experimental thrombin production curves found in [Lawson, Kalafatis et
247 al. 1994] (Figure 5).

248 The next test (Case 4) involved adjusting the model constants in order to fit an arbitrary
249 thrombin generation curve. The experimental curve was found in [Hemker, Giesen et al.
250 2003]. Figure 6, shows that the model predicts the experimental curve with good accuracy.
251 For future application of the model under flow conditions characterised by non-uniform
252 concentrations of platelets, it has been considered important to test its behaviour with given
253 constants for varying concentration of platelets near to the physiological values. We adjusted
254 the constants so that the model approximated the TGA results for platelet concentration 150×10^9
255 pl/L (physiological values are $200\text{-}400 \times 10^9 \text{pl/L}$) and then applied the model with the
256 same setup for two other values of platelet concentrations; Cases 5-7 use the same values for
257 reaction rate constants with platelet concentration 400 , 150 and $100 \times 10^9 \text{pl/L}$ respectively.
258 The results shown on Table 3 are within the range of values reported in [Gerotziafas, Depasse
259 et al. 2005] although the dependence of maximum concentration of thrombin on platelet
260 concentration seems a little stronger than for the in vitro experiments. The resulting curves
261 are shown in Figure 3. Further increase of platelet concentration resulted in higher values for
262 maximum thrombin concentration and small decrease of T_{max} , without significant effect on
263 ETP. If the constants describing platelet activation are also suitably modified, the equations
264 can match curves that depict slower thrombin formation like the ones reported in [Allen,

265 Wolberg et al. 2004] for lower platelet concentrations (75×10^9 pl/L) as shown in Figure 4.
266 The values of the model constants after modification, in order to fit different cases, are shown
267 in Table 4 and for all cases the values are within a reasonable range.

268 **Discussion**

269 This work presents a phenomenological model for thrombin generation that is flexible
270 enough to reproduce a wide range of cases and simple enough to be used for modelling
271 thrombin generation in large scale CFD simulations – in contrast with the most recently
272 suggested models. The four equations of the model are based on the principle assumption that
273 all reactions occur either on the platelet surface or on the reacting site of the vessel wall.

274 The reactions related to platelet activation actually represent the transition from the initiation
275 to the propagation phase. As the curves used to reproduce a wide range of TGA results
276 correspond to different experiments, these constants vary significantly between two groups of
277 Cases. In the experiments for Cases 1-4, where phospholipids have been used as a substrate
278 for enzymatic reactions, this transition is much faster than for Cases 5-8 where human
279 platelets have been used. For Cases 5-8 the values of these constants have been adjusted
280 manually. It is interesting that the calculated time until platelets reach half of the maximum
281 activity for Case 8 is 5-10 min, in agreement with [Allen, Wolberg et al. 2004]. However, as
282 reported recently [Ninivaggi, Apitz-Castro et al. 2012], TGA results in whole blood resemble
283 the curves of Case 1 and 4, (possibly because red blood cells that are not included in most
284 TGA also contribute to thrombin generation [Ninivaggi, Apitz-Castro et al. 2012; Whelihan
285 and Mann 2013]) so this modification of the parameters related to platelet activation is not
286 necessary for physiological cases and the model can be calibrated as described above. On the
287 other hand with the use of this modification the model could also approximate pathological
288 cases as haemophilia or thrombin generation after anticoagulation treatment. In contrast to

289 the methods described and reviewed in [Brummel-Ziedins 2013] where the effect of the
290 variation of each factor concentration and activity is investigated, this model uses only the
291 information included in the TGA curve, thus it has some limitations. For a given value of
292 inhibition reaction rate, has a maximum lag time that it can reproduce if the reported lag time
293 is greater than this maximum value, modification of the inhibition constant is required.

294 Curves corresponding to pathological situations as severe haemophilia A [Wagenvoord,
295 Hemker et al. 2006]) can be approximated. As factor VIII is mainly involved in the
296 propagation phase, it is expected that in order to reproduce curves for different fVIII
297 concentrations the related constants (k_{in} , k_{AP}^{IIa} and k_{IIa}^{AP}) should be modified. As shown in
298 Figure 8, this can be done (the concentrations of VIII have been calculated using 12.8 hours
299 as half-life of fVIII [van Dijk, van der Bom et al. 2005]). At first sight, the most significant
300 inaccuracy of the model (when the initial values of the parameters are used) is that the time
301 interval between the initiation of thrombin burst and maximum concentration of thrombin is
302 smaller than the one reported in TGAs (2.8min compared to 2min predicted by the model)
303 when adjusting only the three previously mentioned parameters. The increase of thrombin
304 concentration predicted by the model is sharper compared to the experimental data and the
305 shapes of the two curves differ for this time interval. That can be fixed by adjusting manually
306 the constants related to platelet activation as we did for Cases 4-8. However the experimental
307 data, while in all studies presented in the form of curves, in some cases actually correspond to
308 measurements in discrete time intervals and the resulting curves are obtained through data
309 fitting. In Figure 7 a plot of three curves is shown, for the time interval of thrombin
310 concentration increase, obtained from the same model results. In one case (dense) the time
311 interval between two data points is 2s, while for the other two cases (sparse1 and sparse2) is
312 30s and 20s respectively –reasonable time intervals between the withdrawal of two samples.
313 It is obvious that curve fitting on experimental values, used in studies prior to the introduction

314 of continuous monitoring of thrombin generation, while making the results more presentable
 315 can also give incorrect information on the actual evolution of the process between two
 316 measurements, so differences between modelled and experimental curves do not necessary
 317 indicate inadequacy of the model.

318 The constant that represents the initial thrombin production rate k_{surf} (for a given value of the
 319 inhibition rate) is mainly determined by the lag time. While there is dependence of different
 320 experiments' results on the exact composition of the samples and the triggering substance
 321 used, for the case described in [van't Veer and Mann 1997; Gerotziafas, Depasse et al. 2005],
 322 there seems to be a clear relationship ($R^2=0.989$) between TF concentration and k_{surf} for the
 323 same experimental conditions and TF concentrations between 1 and 30pM:

$$k_{surf} = k_{surf,max} \left(A + B \ln \left(\frac{[TF]}{[TF_{max}]} \right) \right)$$

324 The constant values are $A = 0.996 \approx 1$, $B = 0.0372$ while for the aforementioned study the
 325 maximum calculated value for the rate of thrombin generation during the initiation phase is
 326 $k_{surf,max} = 7.91 \cdot 10^{-6} s^{-1}$ and the relationship can approximately be written as:

$$k_{surf} = k_{surf,max} \left(1 + 0.0372 \cdot \ln \left(\frac{[TF]}{[TF_{max}]} \right) \right)$$

327 These relationship gives good result when estimating k_{surf} in other studies with similar
 328 methodology, but for studies using recombinant TF:VIIa as trigger for the coagulation
 329 process, while the a good correlation between k_{surf} and trigger concentration can be
 330 established, ($R^2>0.98$) the resulting formulas are different.

331 For the case of thrombus formation on a reacting site of a blood vessel wall, the term
 332 representing the slow phase of thrombin generation corresponds to a surface reaction term.

333 The reaction rate for the surface reaction can be calculated with the use of the reported
334 surface TF concentration in atheromatous plaques ($33\text{pg}/\text{cm}^2$) [Bonderman, Teml et al. 2002]
335 and the molecular weight of (46,000Da approximately [Arabinda Guha 1986]). For a
336 computational cubic cell of e.g. $100\mu\text{m}$ this numbers would lead to a TF concentration of
337 about 70pM resulting to $k_{surf} = 9.75 \cdot 10^{-6}\text{s}^{-1}$. Sub-threshold concentration of thrombin
338 actually represents also the products of the previous steps of coagulation. At the same time
339 this approach allows a slow rate of fibrin production before the burst of thrombin and a
340 realistic prediction of clotting time. As TGA results demonstrate inter-laboratory variation
341 [Van Veen, Gatt et al. 2008], this model, based on TGA results and with its simplified
342 character, does not claim to reproduce with precise accuracy thrombin generation but offers a
343 way to model thrombin generation that (1) has comparative value, in the sense that it can be
344 adjusted to describe different rates of thrombin generation, and (2) can be easily coupled with
345 CFD simulations. We believe that these equations, if combined with two more, one
346 describing fibrin formation and one describing platelet deposition on the reacting site of the
347 vessel, can be used as a thrombus formation model for three dimensional CFD simulations in
348 blood vessels. The results of such a model can be used to compare the evolution of thrombus
349 formation in different cases and for different thrombogenic potential of human blood. Finally,
350 as the model describes the production of thrombin in blood in a phenomenological way, it
351 does not require additional information regarding the concentration of different factors and
352 the details for every reaction in the coagulation system and it can be calibrated and applied
353 directly for different cases based only on the parameters or the curve of the TGA (or the
354 curve itself).

355 **Declarations**

356 Competing interests: None declared

357 Funding: None

358 Ethical approval: Not required

359

360 (4,585 words)

361 **References**

- 362 Allen, G., A. Wolberg, et al. (2004). "Impact of procoagulant concentration on rate, peak and
363 total thrombin generation in a model system." Journal of Thrombosis and
364 Haemostasis **2**(3): 402-413.
- 365 Anand, M., K. Rajagopal, et al. (2003). "A Model Incorporating some of the Mechanical and
366 Biochemical Factors Underlying Clot Formation and Dissolution in Flowing Blood."
367 Journal of Theoretical Medicine **5**(3-4): 183-218.
- 368 Anand, M., K. Rajagopal, et al. (2005). "A Model for the Formation and Lysis of Blood
369 Clots." Pathophysiology of Haemostasis and Thrombosis **34**(2-3): 109-120.
- 370 Arabinda Guha, R. B., William Konigsberg and Yale Nemerson (1986). "Affinity purification
371 of human tissue factor: Interaction of factor VII and tissue factor in detergent
372 micelles." Biochemistry **83**: 299-302.
- 373 Badimon, L., J. J. Badimon, et al. (1986). "Influence of arterial damage and wall shear rate on
374 platelet deposition. Ex vivo study in a swine model." Arteriosclerosis, Thrombosis,
375 and Vascular Biology **6**(3): 312-320.
- 376 Beltrami, E. and J. Jesty (1995). "Mathematical analysis of activation thresholds in enzyme-
377 catalyzed positive feedbacks: application to the feedbacks of blood coagulation."
378 Proceedings of the National academy of Sciences of the United States of America
379 **92**(19): 8744-8748.
- 380 Bodnár, T. and A. Sequeira (2008). "Numerical simulation of the coagulation dynamics of
381 blood." Computational and Mathematical Methods in Medicine **9**(2): 83-104.
- 382 Bonderman, D., A. Teml, et al. (2002). "Coronary no-reflow is caused by shedding of active
383 tissue factor from dissected atherosclerotic plaque." Blood **99**(8): 2794-2800.
- 384 Brass, L. F. (2003). "Thrombin and Platelet Activation*." CHEST Journal **124**(3_suppl):
385 18S-25S.
- 386 Brummel-Ziedins, K. (2013). "Models for thrombin generation and risk of disease." Journal
387 of Thrombosis and Haemostasis **11**: 212-223.
- 388 Fernández-Ortiz, A., J. J. Badimon, et al. (1994). "Characterization of the relative
389 thrombogenicity of atherosclerotic plaque components: Implications for consequences
390 of plaque rupture." Journal of the American College of Cardiology **23**(7): 1562-1569.
- 391 Fogelson, A. L. and R. D. Guy (2004). "Platelet-wall interactions in continuum models of
392 platelet thrombosis: formulation and numerical solution." Mathematical Medicine and
393 Biology **21**(4): 293-334.
- 394 Fogelson, A. L. and R. D. Guy (2008). "Immersed-boundary-type models of intravascular
395 platelet aggregation." Computer Methods in Applied Mechanics and Engineering
396 **197**(25-28): 2087-2104.
- 397 Fogelson, A. L. and N. Tania (2005). "Coagulation under Flow: The Influence of Flow-
398 Mediated Transport on the Initiation and Inhibition of Coagulation." Pathophysiology

- 399 of Haemostasis and Thrombosis **34**(2-3): 91-108.
- 400 Folie, B. J. and L. V. McIntire (1989). "Mathematical analysis of mural thrombogenesis.
401 Concentration profiles of platelet-activating agents and effects of viscous shear flow."
402 Biophysical Journal **56**(6): 1121-1141.
- 403 Frojmovic, M. M., R. F. Mooney, et al. (1994). "Dynamics of platelet glycoprotein IIb-IIIa
404 receptor expression and fibrinogen binding. I. Quantal activation of platelet
405 subpopulations varies with adenosine diphosphate concentration." Biophysical
406 Journal **67**(5): 2060-2068.
- 407 Frojmovic, M. M., R. F. Mooney, et al. (1994). "Dynamics of platelet glycoprotein IIb-IIIa
408 receptor expression and fibrinogen binding. II. Quantal activation parallels platelet
409 capture in stir-associated microaggregation." Biophysical Journal **67**(5): 2069-2075.
- 410 Furie, B. and B. C. Furie (2008). "Mechanisms of Thrombus Formation." New England
411 Journal of Medicine **359**(9): 938-949.
- 412 Gerotziapas, G. T., F. Depasse, et al. (2005). "Towards a standardization of thrombin
413 generation assessment: The influence of tissue factor, platelets and phospholipids
414 concentration on the normal values of Thrombogram-TrombinoScope assay."
415 Thrombosis Journal **3**(16).
- 416 Gibson, C. M., L. Diaz, et al. (1993). "Relation of vessel wall shear stress to atherosclerosis
417 progression in human coronary arteries." Arteriosclerosis, Thrombosis, and Vascular
418 Biology **13**(2): 310-315.
- 419 Hemker, H. C. and S. Béguin (1995). "Thrombin generation in plasma: its assessment via the
420 endogenous thrombin potential." Thrombosis and haemostasis **74**(1): 134-138.
- 421 Hemker, H. C., P. Giesen, et al. (2003). "Calibrated automated thrombin generation
422 measurement in clotting plasma." Pathophysiology of Haemostasis and Thrombosis
423 **33**(1): 4-15.
- 424 Hockin, M. F., K. C. Jones, et al. (2002). "A Model for the Stoichiometric Regulation of
425 Blood Coagulation." Journal of Biological Chemistry **277**(21): 18322-18333.
- 426 Hoffman, M. and D. M. Monroe (2001). "A cell-based model of hemostasis." Thrombosis
427 and haemostasis **85**(6): 958-965.
- 428 Hubbell, J. A. and L. V. McIntire (1986). "Platelet active concentration profiles near growing
429 thrombi. A mathematical consideration." Biophysical Journal **50**(5): 937-945.
- 430 Jesty, J., W. Yin, et al. (2003). "Platelet activation in a circulating flow loop: combined
431 effects of shear stress and exposure time." Platelets **14**(3): 143-149.
- 432 Jones, K. C. and K. G. Mann (1994). "A model for the tissue factor pathway to thrombin. II.
433 A mathematical simulation." Journal of Biological Chemistry **269**(37): 23367-23373.
- 434 Kuharsky, A. L. and A. L. Fogelson (2001). "Surface-Mediated Control of Blood
435 Coagulation: The Role of Binding Site Densities and Platelet Deposition."
436 Biophysical Journal **80**(3): 1050-1074.
- 437 Lai, M.-C. and C. S. Peskin (2000). "An Immersed Boundary Method with Formal Second-
438 Order Accuracy and Reduced Numerical Viscosity." Journal of Computational
439 Physics **160**(2): 705-719.
- 440 Lawson, J. H., M. Kalafatis, et al. (1994). "A model for the tissue factor pathway to thrombin.
441 I. An empirical study." Journal of Biological Chemistry **269**(37): 23357-23366.
- 442 Leiderman, K. and A. L. Fogelson (2011). "Grow with the flow: a spatial-temporal model of
443 platelet deposition and blood coagulation under flow." Mathematical Medicine and
444 Biology **28**(1): 47-84.
- 445 Liu, L., J. Freedman, et al. (1994). "Thrombin binding to platelets and their activation in
446 plasma." British Journal of Haematology **88**(3): 592-600.
- 447 Lo, K., W. S. Denney, et al. (2005). "Stochastic Modeling of Blood Coagulation Initiation."
448 Pathophysiology of Haemostasis and Thrombosis **34**(2-3): 80-90.

- 449 Marée, A. M., V. Grieneisen, et al. (2007). The Cellular Potts Model and Biophysical
 450 Properties of Cells, Tissues and Morphogenesis. Single-Cell-Based Models in
 451 Biology and Medicine. A. A. Anderson, M. J. Chaplain and K. Rejniak, Birkhäuser
 452 Basel: 107-136.
- 453 Monroe, D. M., M. Hoffman, et al. (2002). "Platelets and Thrombin Generation."
 454 Arteriosclerosis, Thrombosis, and Vascular Biology **22**(9): 1381-1389.
- 455 Mosesson, M. W. (2005). "Fibrinogen and fibrin structure and functions." Journal of
 456 Thrombosis and Haemostasis **3**(8): 1894-1904.
- 457 Nesbitt, W. S., E. Westein, et al. (2009). "A shear gradient-dependent platelet aggregation
 458 mechanism drives thrombus formation." Nat Med **15**(6): 665-673.
- 459 Ninivaggi, M., R. Apitz-Castro, et al. (2012). "Whole-Blood Thrombin Generation Monitored
 460 with a Calibrated Automated Thrombogram-Based Assay." Clinical Chemistry **58**(8):
 461 1252-1259.
- 462 Okorie, U. M., W. S. Denney, et al. (2008). "Determination of surface tissue factor thresholds
 463 that trigger coagulation at venous and arterial shear rates: amplification of 100 fM
 464 circulating tissue factor requires flow." Blood **111**(7): 3507-3513.
- 465 Oliver, J. A., D. M. Monroe, et al. (1999). "Thrombin Activates Factor XI on Activated
 466 Platelets in the Absence of Factor XII." Arteriosclerosis, Thrombosis, and Vascular
 467 Biology **19**(1): 170-177.
- 468 Peskin, C. S. (2002). "The immersed boundary method." Acta Numerica **11**: 479-517.
- 469 Qiao, Y. H., C. Q. Xu, et al. (2004). "The kinetic model and simulation of blood coagulation-
 470 the kinetic influence of activated protein C." Medical Engineering & Physics **26**(4):
 471 341-347.
- 472 Rauch, U., J. I. Osende, et al. (2001). "Thrombus formation on atherosclerotic plaques:
 473 pathogenesis and clinical consequences." Annals of internal medicine **134**(3): 224-
 474 238.
- 475 Reininger, A. J., I. Bernlochner, et al. (2010). "A 2-Step Mechanism of Arterial Thrombus
 476 Formation Induced by Human Atherosclerotic Plaques." Journal of the American
 477 College of Cardiology **55**(11): 1147-1158.
- 478 Rendu, F. and B. Brohard-Bohn (2001). "The platelet release reaction: granules' constituents,
 479 secretion and functions." Platelets **12**(5): 261-273.
- 480 Rosing, J., J. van Rijn, et al. (1985). "The role of activated human platelets in prothrombin
 481 and factor X activation." Blood **65**(2): 319-332.
- 482 SBtoolbox (2006). "Systems Biology Toolbox for MATLAB: A computational platform for
 483 research in Systems Biology " Bioinformatics and Biology Insights **22**(4): 514-515.
- 484 Shen, F., C. J. Kastrup, et al. (2008). "Threshold Response of Initiation of Blood Coagulation
 485 by Tissue Factor in Patterned Microfluidic Capillaries Is Controlled by Shear Rate."
 486 Arteriosclerosis, Thrombosis, and Vascular Biology **28**(11): 2035-2041.
- 487 Smith, S. A. (2009). "The cell-based model of coagulation." Journal of Veterinary
 488 Emergency and Critical Care **19**(1): 3-10.
- 489 Sorensen, E. N., G. W. Burgreen, et al. (1999). "Computational Simulation of Platelet
 490 Deposition and Activation: I. Model Development and Properties." Annals of
 491 Biomedical Engineering **27**(4): 436-448.
- 492 van't Veer, C. and K. G. Mann (1997). "Regulation of Tissue Factor Initiated Thrombin
 493 Generation by the Stoichiometric Inhibitors Tissue Factor Pathway Inhibitor,
 494 Antithrombin-III, and Heparin Cofactor-II." Journal of Biological Chemistry **272**(7):
 495 4367-4377.
- 496 van Dijk, K., J. G. van der Bom, et al. (2005). "Factor VIII half-life and clinical phenotype of
 497 severe hemophilia A." Haematologica **90**(4): 494-498.
- 498 Van Veen, J., A. Gatt, et al. (2008). "Thrombin generation testing in routine clinical practice:

- 499 are we there yet?" British Journal of Haematology **142**(6): 889-903.
- 500 Wagenvoord, R., P. W. Hemker, et al. (2006). "The limits of simulation of the clotting
501 system." Journal of Thrombosis and Haemostasis **4**(6): 1331-1338.
- 502 Whelihan, M. F. and K. G. Mann (2013). "The role of the red cell membrane in thrombin
503 generation." Thrombosis Research.
- 504 Willems, G., T. Lindhout, et al. (1991). "Simulation Model for Thrombin Generation in
505 Plasma." Pathophysiology of Haemostasis and Thrombosis **21**(4): 197-207.
- 506 Xu, C., X. Hu Xu, et al. (2005). "Simulation of a mathematical model of the role of the TFPI
507 in the extrinsic pathway of coagulation." Computers in Biology and Medicine **35**(5):
508 435-445.
- 509 Xu, Z., N. Chen, et al. (2008). "A multiscale model of thrombus development." Journal of
510 The Royal Society Interface **5**(24): 705-722.
- 511 Xu, Z., N. Chen, et al. (2009). "Study of blood flow impact on growth of thrombi using a
512 multiscale model." Soft Matter **5**(4): 769-779.
- 513 Xu, Z., J. Lioi, et al. (2010). "A Multiscale Model of Venous Thrombus Formation with
514 Surface-Mediated Control of Blood Coagulation Cascade." Biophysical Journal **98**(9):
515 1723-1732.
- 516 Yang, X. S., R. W. Lewis, et al. (2004). "Finite Element Analysis of Fogelson's Model for
517 Platelet Aggregation."
- 518 Zarnitsina, V. I., A. V. Pokhilko, et al. (1996). "A Mathematical model for the spatio-
519 temporal dynamics of intrinsic pathway of blood coagulation. I. The model
520 description." Thrombosis Research **84**(4): 225-236.
- 521 Zarnitsina, V. I., A. V. Pokhilko, et al. (1996). "A Mathematical model for the spatio-
522 temporal dynamics of intrinsic pathway of blood coagulation. II. Results."
523 Thrombosis Research **84**(5): 333-344.

524

525 **Appendix: Equations' solution:**

- 526 a. Under the assumption that all platelets are instantly activated when thrombin reaches
527 its threshold value, the concentration of platelets is zero when thrombin concentration
528 is below the threshold value and equal to the resting platelet concentration when
529 thrombin exceeds the threshold values. The equations describing thrombin and
530 prothrombin concentration become:

$$\frac{\partial [IIa]}{\partial t} = -k_{in}[IIa] + k_{tot} \cdot [II]$$

$$\frac{\partial [II]}{\partial t} = -k_{tot} \cdot [II]$$

- 531 Here k_{tot} represent the total rate of prothrombin conversion to thrombin and includes both the
532 production on the reacting site and on the platelet surfaces:

$$k_{tot} = k_{surf} + k_{II}^{AP} \cdot [PL], \text{ if } [IIa] > [IIa]_{th}$$

$$k_{tot} = k_{surf}, \quad \text{if } [IIa] \leq [IIa]_{th}$$

533 This leads to a direct solution for prothrombin concentration:

$$[II](t) = [II](t = 0) \cdot e^{-k_{tot}t}$$

534 The D.E. describing thrombin concentration becomes:

$$\frac{\partial [IIa]}{\partial t} = -k_{in}[IIa] + k_{tot} \cdot [II]_o \cdot e^{-k_{tot}t}, \text{ or } \frac{dx}{dt} = Ax - CB e^{Ct}$$

$$\text{where } A = -k_{in}, B = [II]_o \text{ and } C = -k_{tot}$$

535 The equation can be rewritten as follows,

$$\frac{dy}{dt} = (A - C) \cdot y - CB, \text{ where } y = x \cdot e^{-Ct}$$

536 The last expression, after manipulation leads to an (approximate because of the aforementioned

537 assumption) analytic solution for the temporal evolution of thrombin concentration (X):

$$X(t) = \frac{e^{Ct}}{A - C} [((A - C)X_0 e^{-Ct_0} - CB)e^{(A-C)t} + CB] \text{ or}$$

$$[IIa](t) = \frac{e^{-k_{tot}t}}{k_{tot} - k_{in}} \left[((k_{tot} - k_{in})[IIa]_0 e^{k_{tot}t_0} + k_{tot} \cdot [II]_o) e^{(k_{tot} - k_{in})t} - k_{tot} \cdot [II]_o \right]$$

538

539 For $[IIa](t = 0) = 0$ the equation gets the simplified form:

$$[IIa](t) = \frac{k_{tot} \cdot [II]_o}{k_{in} - k_{tot}} (e^{-k_{tot}t} - e^{-k_{in}t})$$

540 b. In the case the data from the whole curve is available, there is another way for

541 obtaining the model constants. The reaction rate is obtained by solving (numerically)

542 the last equation:

$$[IIa]_{th} - \frac{k_{surf} \cdot [II]_o}{k_{in} - k_{surf}} (e^{-k_{surf}Tlag} - e^{-k_{in}Tlag}) = 0$$

543 As the activated platelet concentration is approximately,

$$[AP] = [RP](0) \left(1 - e^{-(t-Tlag)k_{AP}^{IIa}}\right), t > Tlag$$

544 Analytical expression can be obtained for prothrombin concentration versus time,

545 $[II](t) = [II](t = 0) \cdot e^{-k_{tot}(t) \cdot t}$ and therefore for the differential equation

546 describing thrombin evolution for $t > Tlag$, $\frac{d}{dt}[IIa] = -k'_{in} \cdot [IIa] + k_{tot}(t) \cdot [II](t)$

547 and the constants can be obtained numerically using an iterative process.

548 List of Figures

549 **Figure 1:** Schematic representation of cell based model for blood coagulation (reproduced

550 from Smith et al 2009). (a) and the reduced model (b). The different coloured arrows

551 represent the actual processes that are lumped in each reaction rate constant. Red:

552 Inhibition of thrombin in plasma by ATIII and near the vessel wall by APC. Green: Platelet

553 activation by thrombin. Purple: thrombin production by activated platelets. Yellow:

554 Thrombin production in plasma near the reacting site on vessel wall, includes all the reactions

555 from binding of VIIa on TF up to the generation of small amounts of Ila and also (mostly) the

556 inhibition of all other species except thrombin. Turquase: Activation of platelets by

557 substances released by activated platelets such as ADP.

558 **Figure 2:** Results of the model for different time steps. For time steps below 0.5s the results

559 coincide.

560 **Figure 3:** Behaviour of the model for different initial platelet concentrations.

561 **Figure 4:** Adjustment of the model in order to reproduce slower thrombin generation,

562 experimental data.¹

563 **Figure 5:** Model results for thrombin production without inhibition, adjusted to fit the results
564 reported in²⁷

565 **Figure 6:** Capability of the model to reproduce an arbitrary thrombin generation curve²⁰

566 **Figure 7:** Dependence of the shape of the curve on the time interval between two data
567 points. While the initial results are the same curve fitting on data produces significantly
568 different curves

569 **Figure 8:** Reproduction of thrombin generation curves corresponding to different fVIII
570 concentrations and the normalized modification of the related constants.

571

572 **Tables, figures**

573 Table 1: Equations of the model

Thrombin (IIa)	$\frac{\partial[IIa]}{\partial t} = -k_{in}[IIa] + (k_{surf} + k_{II}^{AP} \cdot [AP]) \cdot [II]$
Prothrombin (II)	$\frac{\partial[II]}{\partial t} = -(k_{surf} + k_{II}^{AP} \cdot [AP]) \cdot [II]$
Activated Platelets (AP)	$\frac{\partial[AP]}{\partial t} = k_{AP}^{AP} \cdot [AP] \cdot [RP] + k_{AP}^{IIa} \cdot [RP]$
Resting Platelets (RP)	$\frac{\partial[RP]}{\partial t} = -k_{AP}^{AP} \cdot [AP] \cdot [RP] - k_{AP}^{IIa} \cdot [RP]$

574

575 Table 2: Constants and parameters

Process	Constant symbol	Initial value (S.I.)	Reference
Thrombin generation by activated platelets	k_{II}^{AP}	$0.0856 - 1.81s^{-1}$	[Rosing, van Rijn et al. 1985; Sorensen, Burgreen et al. 1999]
Thrombin generation on reacting surface	k_{surf}	$10^{-5}s^{-1}$	n/a
Platelet activation by thrombin	k_{AP}^{IIa}	$0, if [IIa] < [IIa]_{thr}$ $0.5, if [IIa] \geq [IIa]_{thr}$	[Kuharsky and Fogelson 2001]
Platelet activation by activated platelets	k_{AP}^{AP}	$5.24 \cdot 10^{-2}s^{-1}$	[Kuharsky and Fogelson 2001]
Thrombin inhibition*	k_{in}	$1.71 \cdot 10^{-2} - 0.2s^{-1}$	[Hockin, Jones et al. 2002; Leiderman and Fogelson 2011]
Thrombin concentration threshold for platelet activation	$[IIa]_{thr}$	$1.75 - 4.18 \cdot 10^{-8}kg/kg$ (0.5-1.2nM or 0.05-0.12U/ml)	[Rosing, van Rijn et al. 1985]

577 Table 3: Results of the model for different cases

		Tlag (min)	Tmax (min)	Cmax (nM)	ETP (nM·min)
Case 1	experiment	3.6 ± 0.8	7.4±1.8	164±50	1321±330
	model	3.7	6.8	165	1364
Case 2	experiment	1.5	3.5	(1.5·10 ³)	n/a
	model	1.5	4	(1.5·10 ³)	n/a
Case 3	experiment	0.67	2.25	(1.5·10 ³)	n/a
	model	0.65	2.38	(1.5·10 ³)	n/a
Case 4	experiment	3.5	4.8	199	735
	model	3.7	4.6	196	710
Case 5	experiment	5±0.5	11±2.7	161±38	1633±81
	model	5.8	9	190	1718
Case 6	experiment	5.5±0.5	11±0.2	98±40	1316±255
	model	6	9.4	91	1370
Case 7	experiment	5.8±0.7	13±0.9	72±38	1135±300
	model	6	9.6	62	1118
Case 8	experiment	15	27	101	2012
	model	13.3	25.3	102	1934

578

579

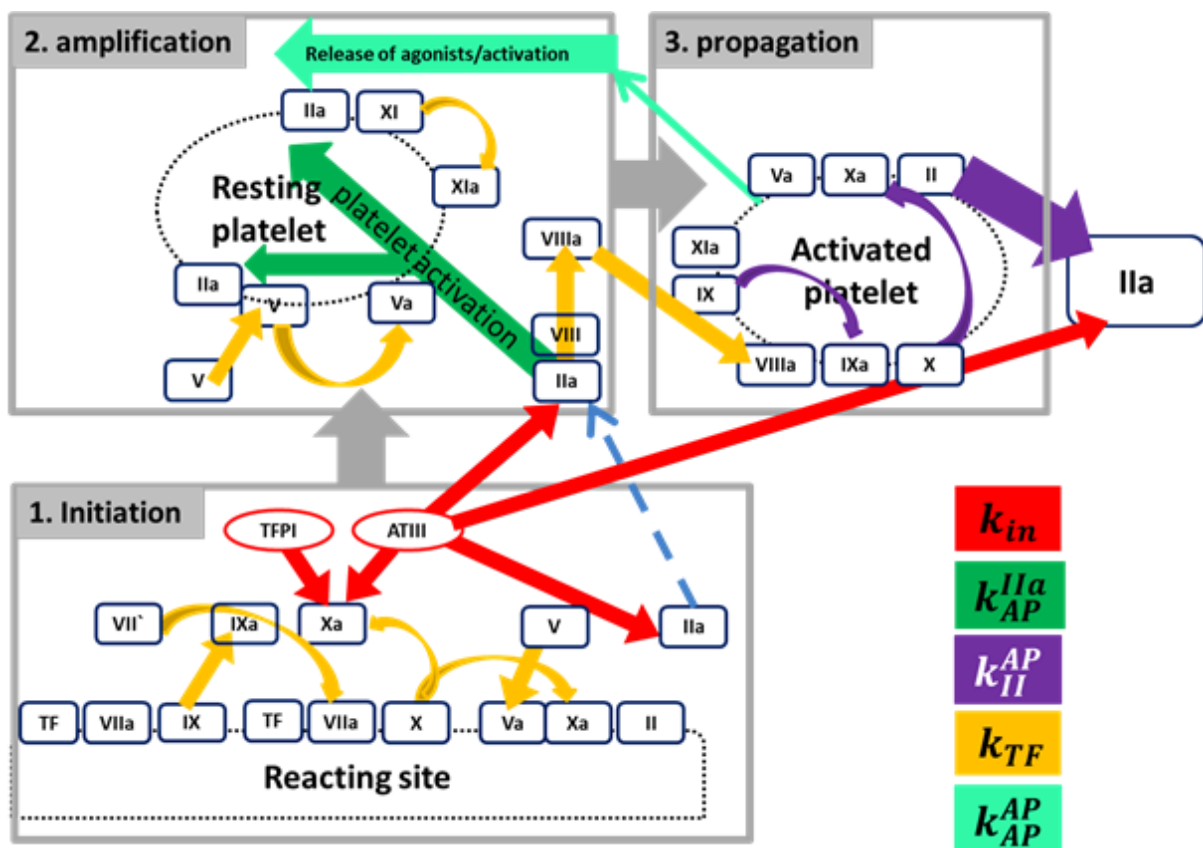
580

581 Table 4: The variation of the model constants after adjustment in order to reproduce different

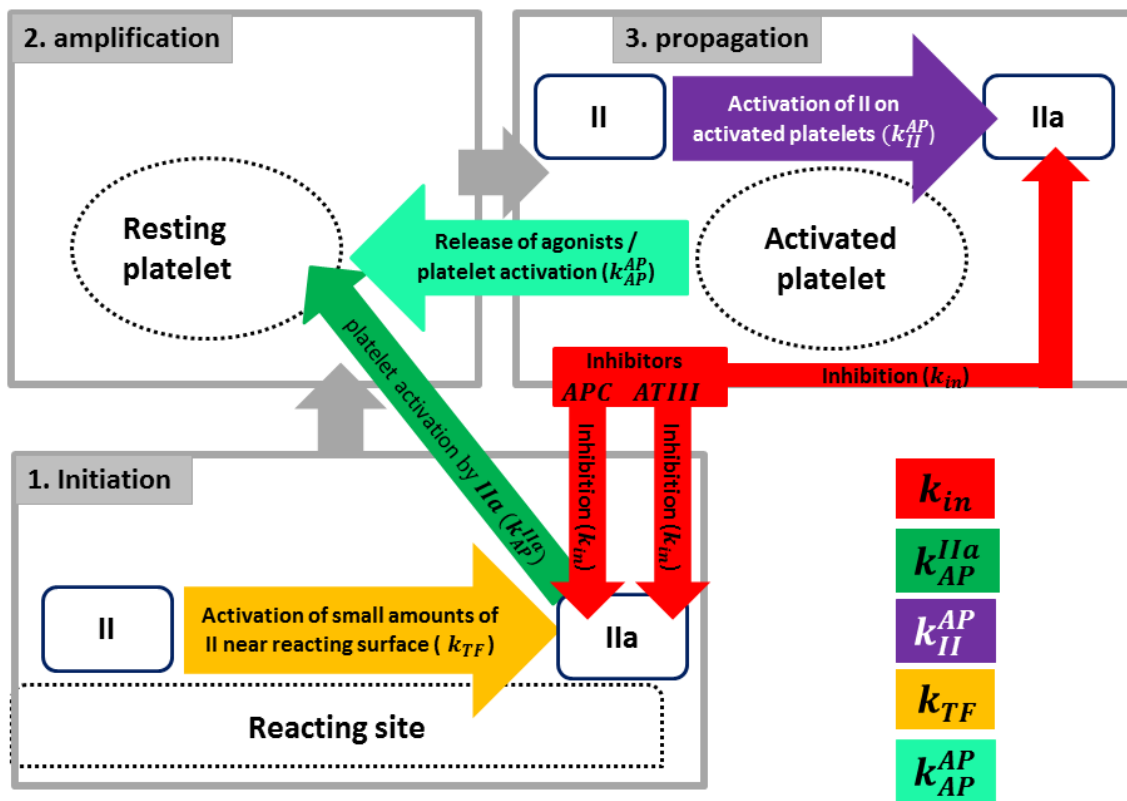
582 cases

Constant	Initial estimations	Case 1	Case 2	Case 3	Case 4	Cases 5-7	Case 8
$k_{surf}(s^{-1})$	10^{-5}	$7.367 \cdot 10^{-6}$	$9.162 \cdot 10^{-6}$	$1.511 \cdot 10^{-5}$	$7.367 \cdot 10^{-6}$	$7.223 \cdot 10^{-6}$	$4.06 \cdot 10^{-7}$
$k_{II}^{AP}(s^{-1})$	0.0856 – 1.81	0.73	2.8	4	1.55	0.525	3.6
$k_{in}(s^{-1})$	$1.71 \cdot 10^{-2}$ – 0.2	0.032	0	0	0.052	0.0262	0.024
$k_{AP}^{IIa}(s^{-1})$	0.2 – 0.5	-	-	0.5	0.5	0.002	0.0018

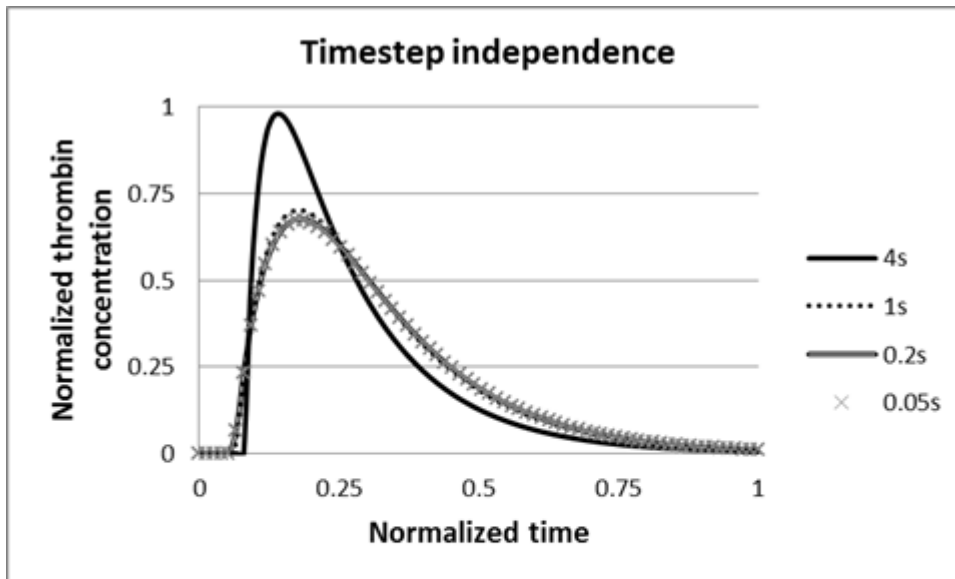
583

584 **Figure 1a**

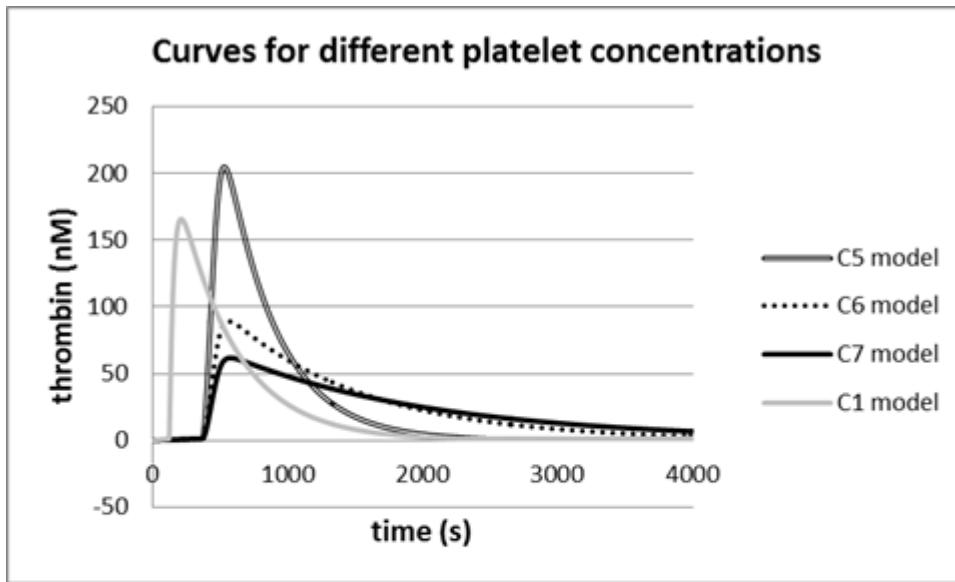
585

586 **Figure 1b**

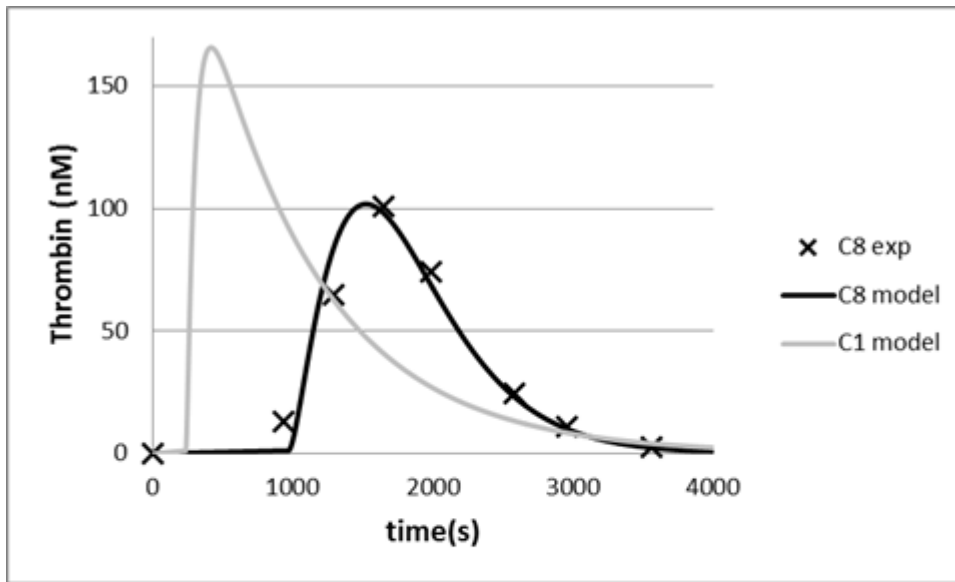
587

588 **Figure 2**

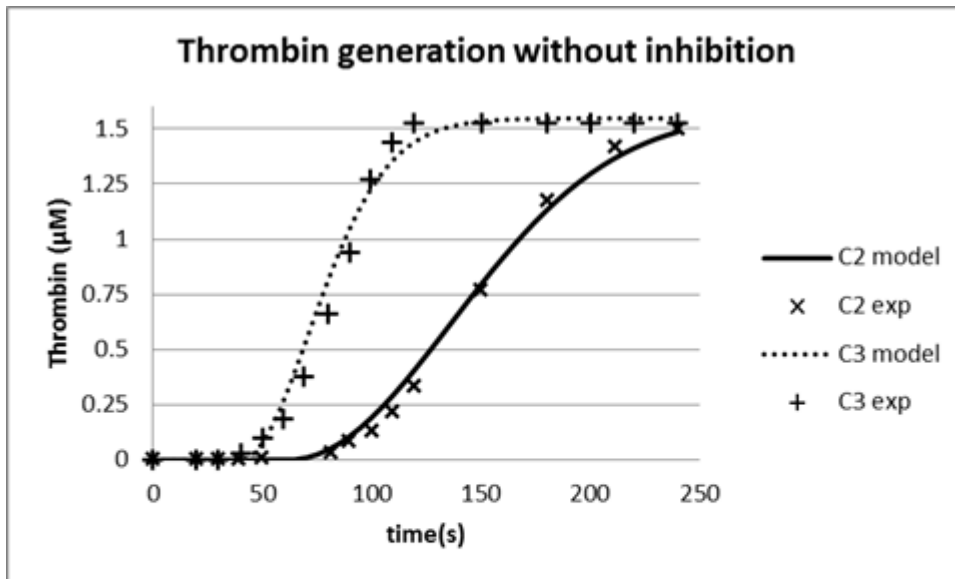
589

590 **Figure 3**

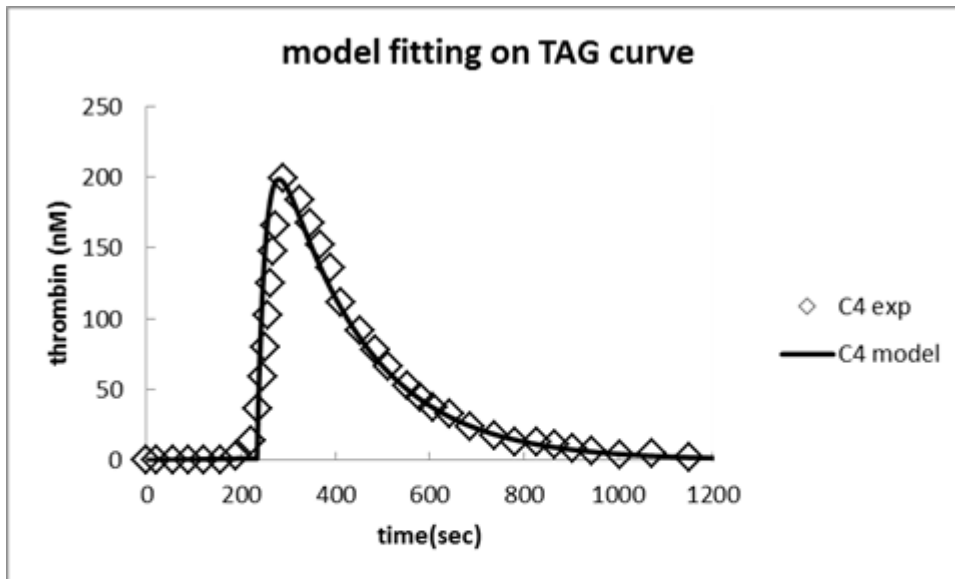
591

592 **Figure 4**

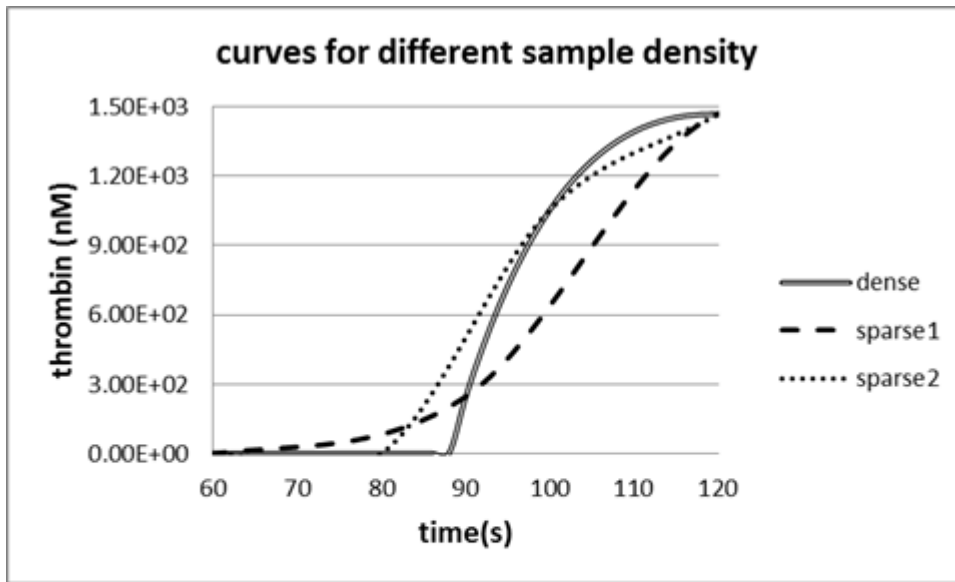
593

594 **Figure 5**

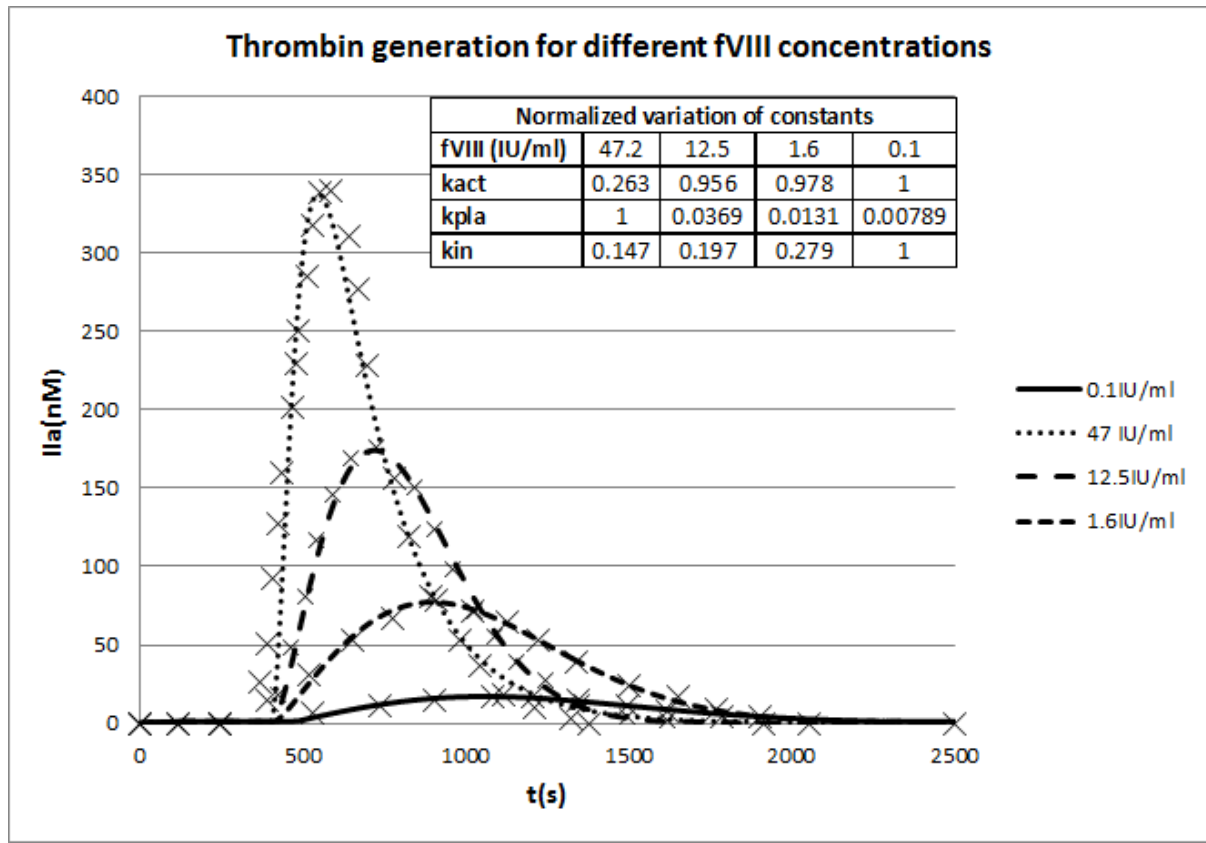
595

596 **Figure 6**

597

598 **Figure 7**

599

600 **Figure 8**

601